

# Synthesis of Alumina- and Alumina/Silica-Coated Titania Particles in an Aerosol Flow Reactor

Quint H. Powell, George P. Fotou,<sup>†</sup> and Toivo T. Kodas\*

Center for Micro-Engineered Ceramics, Department of Chemical and Nuclear Engineering,  
University of New Mexico, Albuquerque, New Mexico 87131

Bruce M. Anderson

Kemira Pigments, Inc., P.O. Box 368, Savannah, Georgia 31402

Received June 11, 1996. Revised Manuscript Received January 7, 1997<sup>®</sup>

In situ coating of titania aerosol particles with alumina and alumina–silica mixtures by chemical vapor deposition, cluster deposition, and sintering was demonstrated in a hot-wall, continuous flow tubular reactor. Titania particles with diameters in the range 0.2–0.8  $\mu\text{m}$  were produced by the reaction of  $\text{TiCl}_4$  with  $\text{O}_2$  at 1300 and 1500  $^\circ\text{C}$  and were passed through a coating region where they were mixed with  $\text{AlCl}_3$  or mixtures of  $\text{AlCl}_3$  and  $\text{SiCl}_4$ . Uniform and dense coatings of  $\text{Al}_2\text{O}_3$  were obtained at both 1300 and 1500  $^\circ\text{C}$  using  $\text{AlCl}_3$  inlet concentrations that corresponded to  $\text{Al}_2\text{O}_3$  mass loading of less than 1 wt %. The coating thickness could be controlled from 5 to 20 nm which corresponded to deposition rates up to 50 nm/s. Uniform and dense coatings of  $\text{Al}_2\text{O}_3/\text{SiO}_2$  were obtained at 1300  $^\circ\text{C}$  when the  $\text{SiO}_2/\text{Al}_2\text{O}_3$  weight ratio was less than 2:1. It is proposed that coating takes place in two modes: (a) chemical vapor deposition of  $\text{AlCl}_3$  and  $\text{SiCl}_4$  on the particle surface and (b) gas-phase reactions of the metal chlorides to form  $\text{Al}_2\text{O}_3$ ,  $\text{SiO}_2$ , or  $\text{Al}_2\text{O}_3/\text{SiO}_2$  particles that subsequently collide with the titania particles and sinter into the coating.

## Introduction

Coated materials are receiving increased attention because of their importance for both a fundamental understanding of their properties and for their applications.<sup>1</sup> Because of the composition gradient imposed by the coating, the surfaces of these materials may possess completely different characteristics than does the core element. This can be exploited to synthesize materials with unique optical, electronic, magnetic, and mechanical properties. Although the technology for coating rather large substrates (in the centimeter range and above) is well established especially in the microelectronics industry,<sup>2</sup> coating of very small substrates such as submicron particles still remains a technical challenge.

Coatings often change the colloidal stability and dispersability and increase the resistance of particles toward various reactions that can degrade the characteristics of the material.<sup>3</sup> The catalytic activity or chemical reactivity of particles can also be enhanced or suppressed by coating them with appropriate metals or metal oxides.<sup>3–5</sup> This is particularly important in the synthesis of phosphor powders used in flat-panel displays and for titania pigments. These and other ap-

plications of these materials mandate that their chemical reactivity is controlled to protect them against degradation induced by various species in plasmas, electrons, and UV photons, respectively.

The properties of coated materials depend strongly on the methods employed to synthesize these materials. Liquid-phase coating techniques are most frequently used.<sup>3</sup> Although dry or gas-phase coating techniques provide several advantages over liquid processes, they have been barely studied.<sup>5,6</sup> Despite the importance of surface modification of particles, little is known about the phenomena involved during coating formation by gas-phase routes.

In a recent study we examined the formation of silica films on submicron titania particles by the gas-phase and surface reactions of  $\text{SiCl}_4$  and  $\text{O}_2$ .<sup>7,8</sup> The reactant  $\text{SiCl}_4$  was chosen to match the reaction temperature of  $\text{TiCl}_4$ . Typical coating rates with this process were on the order of 10–100 nm/s, which are high compared to film growth rates normally obtained by other coating processes.<sup>2</sup> The coating morphology depended strongly on reaction conditions. This was attributed to the interplay of different film-formation processes including chemical vapor deposition, gas-phase silica particle formation, coagulation with  $\text{TiO}_2$  particles, and sintering. A theoretical study that followed supported the qualitative interpretation of the experimental findings.<sup>9</sup> This study showed that coating characteristics depended on the relative rates of gas-phase and surface reaction

\* To whom correspondence should be addressed: E-mail: [ttkodas@unm.edu](mailto:ttkodas@unm.edu).

<sup>†</sup> Presently at Cabot Corp., Tuscola, IL 61953.

<sup>®</sup> Abstract published in *Advance ACS Abstracts*, February 15, 1997.

(1) Chediak, J. A. *J. Am. Ceram. Soc. Bull.* **1996**, *75*, 52.

(2) Kodas, T. T.; Hampden-Smith, M. *The Chemistry of Metal CVD*; VCH: Weinheim, 1994.

(3) Braun, J. H.; Baidins, A.; Marganski, R. E. *Prog. Org. Coatings* **1992**, *20*, 105.

(4) Papp, J.; Shen, H.-S.; Keshaw, K.; Dwight, K.; Wold, A. *Chem. Mater.* **1993**, *5*, 284.

(5) Santacesaria, E.; Carra, S.; Pace, R. C.; Scotti, C. *Ind. Eng. Chem. Prod. Res. Dev.* **1982**, *21*, 496.

(6) Santacesaria, E.; Carra, S.; Pace, R. C.; Scotti, C. *Ind. Eng. Chem. Prod. Res. Dev.* **1982**, *21*, 501.

(7) Powell, Q. H.; Kodas, T. T.; Anderson, B. A. *CVD J.* **1996**, *2*, 179.

(8) Powell, Q. H.; Fotou, G. P.; Kodas, T. T.; Anderson, B. A.; Guo, Y. *J. Mater. Res.* **1997**, *12*.

(9) Jain, S.; Fotou, G. P.; Kodas, T. T. *J. Colloid Interface Sci.* **1997**, *185*, 26.

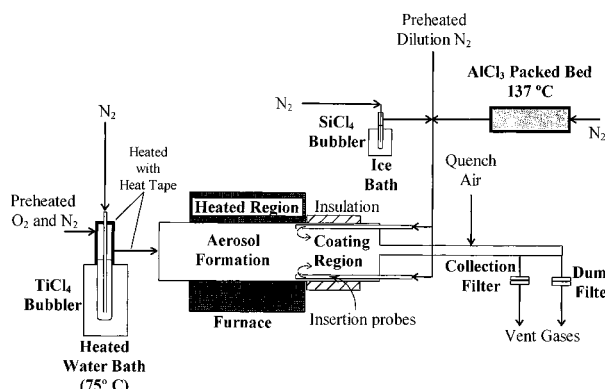


**Figure 1.** Schematic of experimental apparatus used for coating titania with  $\text{Al}_2\text{O}_3$  and  $\text{Al}_2\text{O}_3/\text{SiO}_2$ .

of the coating reactants which in turn were influenced by process parameters such as reactor temperature and coating reactant concentration.

These previous studies focused only on the single-reactant ( $\text{SiCl}_4$ )  $\text{SiO}_2$ - $\text{TiO}_2$  system. The goal of the present study is to identify and understand the overall pathway for coating particles by gas-phase reactions from a more general perspective with two gaseous reactants. For this purpose we investigated the formation of alumina and alumina/silica coatings on titania aerosol particles starting from their chlorides. The metal chlorides were used to match the reaction temperature of  $\text{TiCl}_4$  and because they are less expensive than metal alkoxides at an industrial scale. This study proposes for the first time a mechanism for coating of aerosol particles with two or more reactants. We show also that dense coatings of silica can be obtained at much lower temperatures than in previous work by adding a source of  $\text{Al}_2\text{O}_3$ .

### Experimental Section

The experimental system used in this study is shown in Figure 1. It is essentially the same system used in previous studies<sup>8</sup> but modified to allow for introduction of the  $\text{Al}_2\text{O}_3$  coating precursor. Titanium tetrachloride vapor was generated by bubbling 2.2 L/min of  $\text{N}_2$  gas (TriGas, 99.9%) through a 100 mL graduated bubbler filled with liquid  $\text{TiCl}_4$  (Aldrich, 99.8%). The temperature of the  $\text{TiCl}_4$ -containing bubbler was maintained at 75 °C using a heated water bath. The  $\text{N}_2/\text{TiCl}_4$  stream coming out of the bubbler was mixed with a combined stream of  $\text{O}_2$  (TriGas, 99.9%) and  $\text{N}_2$  heated at 85 °C. The oxygen and nitrogen inlet gas volumetric flow rates were both controlled at 3 L/min each. In all coating experiments, the delivery rate of  $\text{TiCl}_4$  to the reactor was determined by recording the volume of  $\text{TiCl}_4$  consumed in each run. This delivery rate was held constant at approximately 30 g/h of  $\text{TiO}_2$ . The combined  $\text{N}_2/\text{TiCl}_4$ - $\text{O}_2$  stream was introduced into the reactor which consisted of a 7.94 cm (inside diameter), 152 cm long, mullite tube (Coors Ceramics) heated externally using an electrically heated furnace (Lindberg) with a 1500 °C, three-zone, 91 cm long heating region. At the exit of the furnace, a 19 cm long section of the mullite reactor tube was insulated to maintain high gas temperatures and to lengthen the coating region.

The coating reactants ( $\text{AlCl}_3$  and  $\text{SiCl}_4$ ) were introduced into the reactor using two opposing 0.64 cm (outside diameter) mullite injection probes. The reactants were injected radially inward at the end of the heated region of the reactor through 0.64 cm long slits on the injection probes. In all coating experiments the injection probe position and the mixing configuration of the gas streams were the same.

For coatings of  $\text{TiO}_2$  with  $\text{Al}_2\text{O}_3$ ,  $\text{AlCl}_3$  vapor was used as the coating precursor. It was generated by vaporizing  $\text{AlCl}_3$

**Table 1.** Experimental Conditions Employed in Coatings of  $\text{TiO}_2$  with  $\text{Al}_2\text{O}_3$

reactor temp, °C	$\text{N}_2$ flow rate through the $\text{AlCl}_3$ generator, L/min	dilution $\text{N}_2$ flow rate, L/min	$\text{Al}_2\text{O}_3$ wt %
1300	0.2	3.0	0.6
1300	0.3	3.0	0.8
1300	0.4	3.0	2.0
1300	1.0	3.0	5.0
1500	0.2	3.0	0.7
1500	0.2	5.0	0.8
1500	1.0	3.0	10.0
1500	1.0	5.0	10.0

powder (Aldrich, 99.9%) inside an externally heated Pyrex tube packed with 4 mm glass beads. The temperature of the  $\text{AlCl}_3$  packed bed was controlled at 137 °C. The resulting  $\text{AlCl}_3$  vapor was transported by passing  $\text{N}_2$  gas at controlled flow rates that varied from 0.2 to 1.0 L/min through the  $\text{AlCl}_3$ -packed bed. This  $\text{N}_2/\text{AlCl}_3$  stream was mixed with a dilution  $\text{N}_2$  gas stream at flow rates of 3 and 5 L/min prior to the injection probes. Table 1 summarizes the conditions under which the  $\text{TiO}_2/\text{Al}_2\text{O}_3$  coating experiments were conducted. The reactor temperature was set at 1300 and 1500 °C. The amount of  $\text{AlCl}_3$  introduced into the reactor was determined from calibration runs of the  $\text{AlCl}_3$  sublimator. This was accomplished by passing carrier  $\text{N}_2$  gas at various flow rates through the heated  $\text{AlCl}_3$ -packed bed, introducing the  $\text{N}_2/\text{AlCl}_3$  stream inside the reactor under the same reactor conditions used in the coating experiments and collecting and weighing the product  $\text{Al}_2\text{O}_3$  powder. The weight fraction of  $\text{Al}_2\text{O}_3$  relative to  $\text{TiO}_2$  calculated based on inlet amounts varied from 0.6 to 10 wt % as shown in Table 1.

For coatings of  $\text{TiO}_2$  with mixtures of  $\text{Al}_2\text{O}_3$  and  $\text{SiO}_2$ ,  $\text{SiCl}_4$  vapor was generated by passing  $\text{N}_2$  gas at 0.03 L/min through a bubbler filled with liquid  $\text{SiCl}_4$  (Aldrich, 99.9%) and kept at 0 °C using an ice-water bath. The amount of  $\text{SiCl}_4$  introduced was determined by measuring the volume change over time of the  $\text{SiCl}_4$  liquid inside the bubbler. The  $\text{N}_2/\text{SiCl}_4$  stream was mixed with the  $\text{N}_2/\text{AlCl}_3$  stream before introduction into the reactor through the injection probes as shown in Figure 1. Table 2 lists the conditions employed in these experiments. The reactor temperature was set at 1300 °C. The flow rate of the  $\text{N}_2/\text{AlCl}_3$  stream was varied from 0.2 to 1.0 L/min, and the dilution  $\text{N}_2$  gas flow rate was 3.0 L/min. Under these conditions, the  $\text{SiO}_2$  to  $\text{Al}_2\text{O}_3$  weight ratio varied from 1 to 10 and the combined weight fraction of  $\text{SiO}_2$  and  $\text{Al}_2\text{O}_3$  relative to  $\text{TiO}_2$  in the powders varied from 0.2 to 4.0 wt % as was calculated from the inlet amounts. The powders produced in the manner described above were collected on 142 mm, 0.45  $\mu\text{m}$  pore size, Tuffryn filters contained in a stainless steel filter holder (Gelman). A second similar filter was used during startup and shutdown of the system to avoid collection of powder produced at transient conditions. In all experiments the dilution nitrogen gas streams were preheated before being mixed with the precursor streams to avoid condensation of the chloride vapors in the transfer lines.

The phase composition of the product powders was determined by X-ray diffraction (XRD) using a Siemens 5000,  $\text{Cu K}\alpha$  diffractometer. The overall morphologies of the coated and uncoated titania particles were obtained by scanning electron microscopy (SEM) using a Hitachi Model S-800 field emission instrument. Transmission electron microscopy (TEM, JEOL JEM 2000 FX and JEOL JEM 2010) was used to obtain information about the morphology and the thickness of the coatings. Energy-dispersive spectroscopy (EDS) using a JEOL JEM 2010 microscope equipped with an Oxford Link ISIS was used to verify the presence of  $\text{SiO}_2$  and/or  $\text{Al}_2\text{O}_3$  on the titania surfaces.

### Results

**Alumina Coatings.** Titania particles produced under the reactor conditions employed in this study were anatase-rich (87 wt % anatase) at 1300 °C and rutile-

**Table 2. Experimental Conditions Employed in Coatings of TiO<sub>2</sub> with Al<sub>2</sub>O<sub>3</sub>/SiO<sub>2</sub>**

reactor temp, °C	N <sub>2</sub> flow rate through the AlCl <sub>3</sub> generator, L/min	N <sub>2</sub> flow rate through the SiCl <sub>4</sub> bubbler, L/min	dilution N <sub>2</sub> flow rate, L/min	SiO <sub>2</sub> /Al <sub>2</sub> O <sub>3</sub> weight ratio
1300	0.2	0.03	3.0	10:1
1300	0.3	0.03	3.0	6:1
1300	0.4	0.03	3.0	2:1
1300	1.0	0.03	3.0	1:1

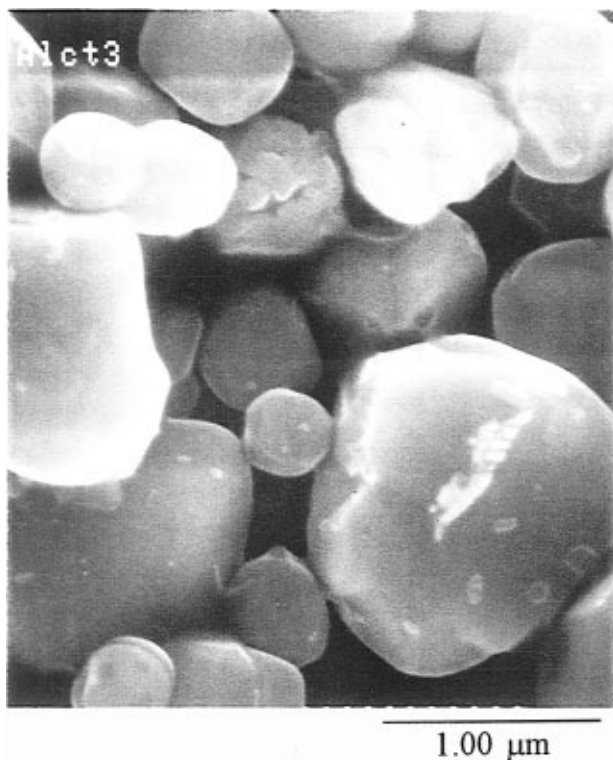


**Figure 2.** SEM showing the surface roughness of alumina-coated titania particles observed at high Al<sub>2</sub>O<sub>3</sub> loading. These particles were produced at 1500 °C using 3 L/min dilution N<sub>2</sub> and 10.0 wt % Al<sub>2</sub>O<sub>3</sub> based on inlet conditions.

rich (80 wt % rutile) at 1500 °C as found by XRD analysis. They had similar morphologies at both temperatures and were polyhedral in shape with well-defined edges and diameters in the range 0.2–0.8 μm.<sup>8</sup>

SEM observations of titania particles coated with Al<sub>2</sub>O<sub>3</sub> at both 1300 and 1500 °C showed the same morphology as uncoated particles. Particles coated at low mass loadings of Al<sub>2</sub>O<sub>3</sub> (<1 wt %) had smooth surfaces at both reactor temperatures. Only when relatively high alumina loadings were used did the surfaces appear to be rougher. Figure 2 shows TiO<sub>2</sub> particles coated with Al<sub>2</sub>O<sub>3</sub> at a reactor temperature of 1500 °C and at 10 wt % alumina loading based on inlet concentrations. In comparison with SiO<sub>2</sub>-coated TiO<sub>2</sub> produced under similar conditions, the Al<sub>2</sub>O<sub>3</sub>-coated titania had much smoother surfaces even at the highest AlCl<sub>3</sub> concentrations used.<sup>8</sup>

TEM analysis of particles coated with Al<sub>2</sub>O<sub>3</sub> at 1300 °C revealed that uniform and dense coatings were obtained at low Al<sub>2</sub>O<sub>3</sub> mass loadings (<1 wt %, Figure 3). Under these conditions almost all of the particles were completely coated. However, the coating thickness varied from particle to particle in the range 5–20 nm which corresponds to deposition rates on the order of 50 nm/s. The presence of Al on the TiO<sub>2</sub> surfaces was verified by EDS. Even at the lowest Al<sub>2</sub>O<sub>3</sub> mass loading used in this study (0.6 wt %) almost all of the particles

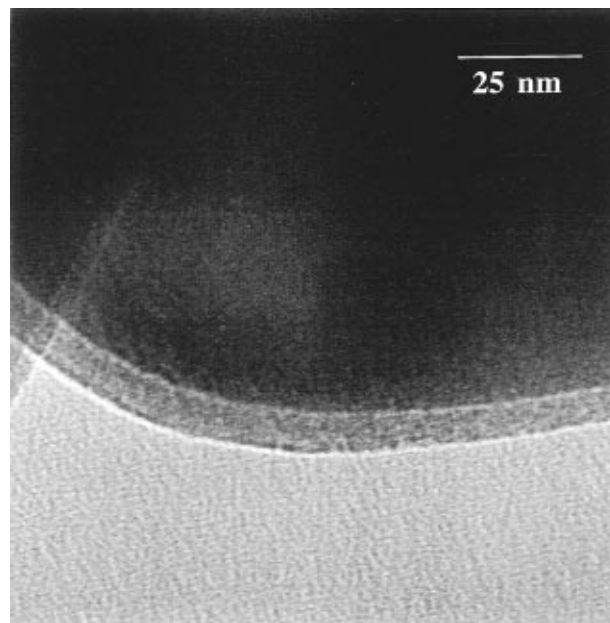


**Figure 3.** Titania particle with a dense Al<sub>2</sub>O<sub>3</sub> coating that was about 10 nm thick and a small section of a particle with a thinner coating that was about 5 nm thick. This powder was made at 1300 °C using 3 L/min dilution N<sub>2</sub> and 0.8 wt % Al<sub>2</sub>O<sub>3</sub>, based on inlet conditions. Almost all of the particles made under these conditions were coated with similar coatings that fully encompassed the particles.

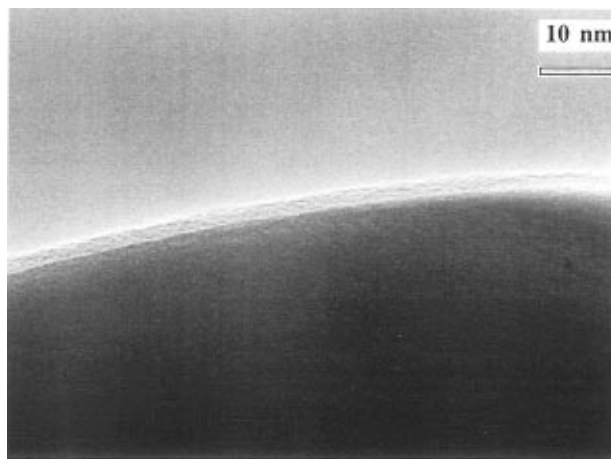


**Figure 4.** Thick (4 nm) Al<sub>2</sub>O<sub>3</sub> coating on TiO<sub>2</sub> particle. This powder was made at 1500 °C using 3 L/min dilution N<sub>2</sub> and 0.8 wt % Al<sub>2</sub>O<sub>3</sub>, based on inlet conditions. Upon comparison to Figure 3, it is evident that coatings obtained at 1500 °C using the same Al<sub>2</sub>O<sub>3</sub> mass loading were similar to the coatings obtained at 1300 °C.

were coated and had similar morphology. A similar behavior was observed at 1500 °C as shown in Figure 4 which is a TEM of a TiO<sub>2</sub> particle coated at 1500 °C and at Al<sub>2</sub>O<sub>3</sub> mass loading of 0.8 wt %. At Al<sub>2</sub>O<sub>3</sub> loadings higher than 1 wt % the TiO<sub>2</sub> particles produced were not completely and uniformly coated at both reactor temperatures. Approximately 50% of the par-

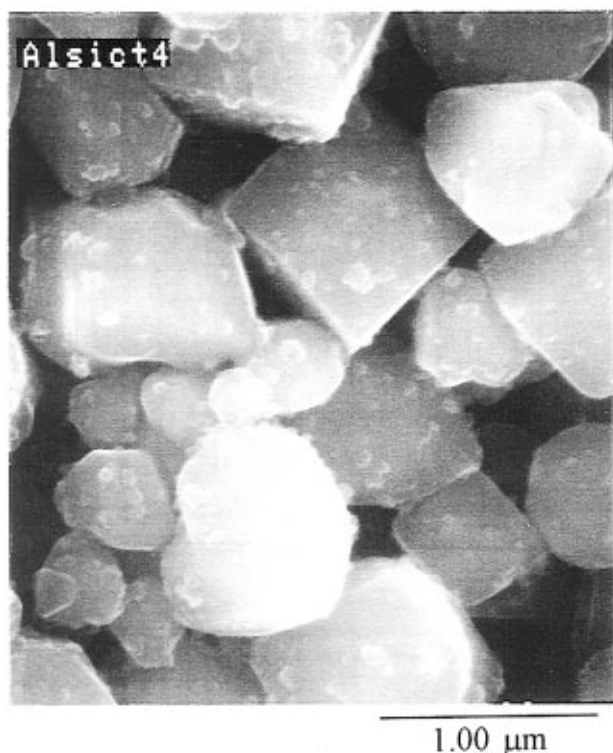


**Figure 5.**  $\text{Al}_2\text{O}_3/\text{SiO}_2$ -coated titania particles showing surface roughness observed at higher amounts of  $\text{Al}_2\text{O}_3$  relative to  $\text{SiO}_2$ . These particles were made at  $1300^\circ\text{C}$  using 3 L/min dilution  $\text{N}_2$  and a  $\text{SiO}_2/\text{Al}_2\text{O}_3$  weight ratio of 1:1, based on inlet conditions.

ticles were not coated, while the rest were partially coated with relatively thick (20–40 nm)  $\text{Al}_2\text{O}_3$  layers. Another important observation was the fact that at  $\text{Al}_2\text{O}_3$  mass loadings higher than 1 wt % and at both reactor temperatures more separate  $\text{Al}_2\text{O}_3$  particles were present in the samples as was verified by EDS. This represented a general trend in the alumina-coated powders: as the  $\text{AlCl}_3$  concentration was increased, fewer particles were coated, more separate  $\text{Al}_2\text{O}_3$  particles were produced, and the coating uniformity decreased. All alumina coatings were X-ray amorphous. Crystalline phases other than anatase and rutile were not detected in the powders. A mass balance on  $\text{Al}_2\text{O}_3$  indicated the majority of the alumina was present in the coating.

**Alumina–Silica Coatings.** Titania particles coated with mixtures of  $\text{SiO}_2$  and  $\text{Al}_2\text{O}_3$  had similar morphology with those coated only with  $\text{Al}_2\text{O}_3$  as found by SEM. Particles coated at high  $\text{SiO}_2/\text{Al}_2\text{O}_3$  weight ratios had smooth surfaces. At lower  $\text{SiO}_2/\text{Al}_2\text{O}_3$  ratios the surface roughness of the particles increased as shown in Figure 5. TEM observations of particles produced under the conditions summarized in Table 2 revealed that coatings were obtained in all cases. Similarly with the pure alumina coating experiments, as the  $\text{Al}_2\text{O}_3$  loading increased fewer coated particles were obtained. Only at the lowest level of  $\text{Al}_2\text{O}_3$  were completely coated titania particles produced. Figure 6a is a typical TEM micrograph of a titania particle coated with a  $\text{SiO}_2/\text{Al}_2\text{O}_3$  layer at a  $\text{SiO}_2/\text{Al}_2\text{O}_3$  weight ratio of 10:1. Figure 6b shows typical EDS spectra from the center and surface of particles coated under these conditions. In this sample all particles had smooth and dense coatings with thicknesses that varied between 3 and 10 nm. Under

these conditions no separate  $\text{SiO}_2$ ,  $\text{Al}_2\text{O}_3$  or composite  $\text{SiO}_2/\text{Al}_2\text{O}_3$  particles were obtained. The  $\text{TiO}_2$  particles were completely coated; however, the coating thickness varied between 20 and 50% on individual particles and from particle to particle in the range 3–10 nm. Increasing further the alumina level (decreasing the  $\text{SiO}_2/\text{Al}_2\text{O}_3$  weight ratio) resulted in particles that were uncoated as well as separate composite  $\text{SiO}_2/\text{Al}_2\text{O}_3$  particles as verified with EDS. Some of these composite particles were loosely attached on the titania particles as shown in Figure 7a. This particular sample consisted of uncoated as well as densely coated particles with average thickness of 10–20 nm. Typical EDS spectra from the center and edge of these particles are shown in Figure 7b. At the highest  $\text{Al}_2\text{O}_3$  loading ( $\text{SiO}_2/\text{Al}_2\text{O}_3$  weight ratio = 1:1) most of the particles were uncoated and more  $\text{SiO}_2/\text{Al}_2\text{O}_3$  separate particles existed in a similar fashion with the pure alumina coatings (Figure 4) as shown in Figure 8a. The presence of both  $\text{SiO}_2$  and  $\text{Al}_2\text{O}_3$  in the coatings was confirmed with EDS as shown in Figure 8b. EDS analysis of separate  $\text{SiO}_2/\text{Al}_2\text{O}_3$  composite particles showed that their  $\text{Al}_2\text{O}_3$  content increased by increasing the inlet concentration of  $\text{AlCl}_3$  or, equivalently, reducing the  $\text{SiO}_2/\text{Al}_2\text{O}_3$  ratio as shown in Figure 9. All coatings were X-ray amorphous. A mass balance of  $\text{SiO}_2$  and  $\text{Al}_2\text{O}_3$  showed most of the silica and alumina were present in the coating.

## Discussion

On the basis of the above observations, possible coating pathways can be proposed for the  $\text{TiO}_2$ – $\text{SiO}_2/\text{Al}_2\text{O}_3$  system and are shown in Figure 10. The gas-phase reactions of  $\text{AlCl}_3$  and/or  $\text{SiCl}_4$  with  $\text{O}_2$  can result in the formation of alumina and silica monomers (path 1). These monomers collide and fuse together to form larger particles of the respective oxides (path 2), their final size depending on temperature and metal chloride concentration. These oxide particles collide with titania particles according to path 3. If the temperature is sufficiently high (fast sintering) or the chloride concentration sufficiently low (fewer and smaller particles) the silica or alumina particles can rapidly sinter on the titania surfaces forming smooth layers of alumina, silica, or alumina/silica mixtures (path 4). Alternatively, the silica and alumina monomers may collide to form aggregates that consist of silica and alumina particles (path 5a). These aggregates may deposit onto titania (path 5b) or may grow by sintering and form mixed  $\text{SiO}_2/\text{Al}_2\text{O}_3$  particles (path 5c) which eventually collide with the titania particles (path 5d). The coating reactants may also directly react on the surfaces of titania particles according to path 6. This reaction path is analogous to film formation on flat surfaces by chemical vapor deposition. It does not involve particle formation, and it normally results in smooth coatings.

Some other processes that are not shown in Figure 10 for simplicity include surface growth of alumina or silica particles formed via paths 1 and 2 by chemical vapor deposition of  $\text{SiCl}_4$  or  $\text{AlCl}_3$  on the surfaces of these particles. Although all of the above pathways for coating formation are likely to take place, some are favored more than others depending on coating reactant concentration and reactivity, temperature and residence time in the reactor, and physical properties of the oxides

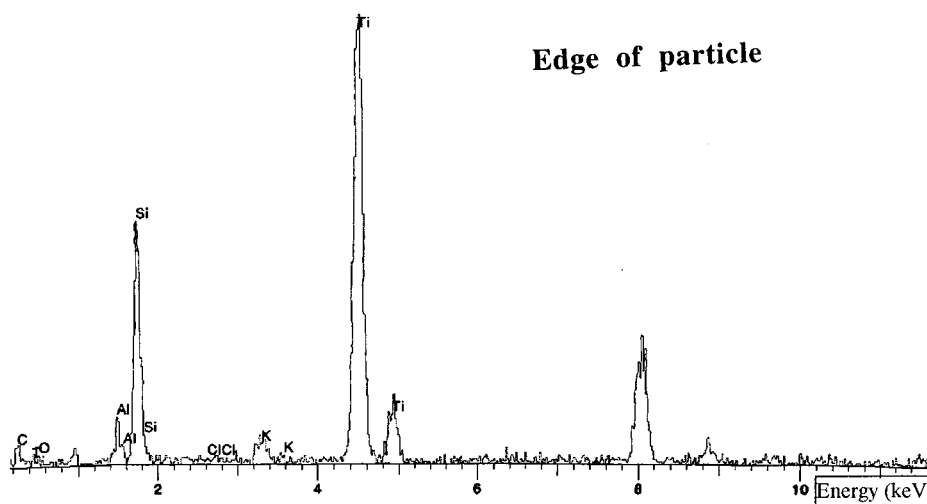
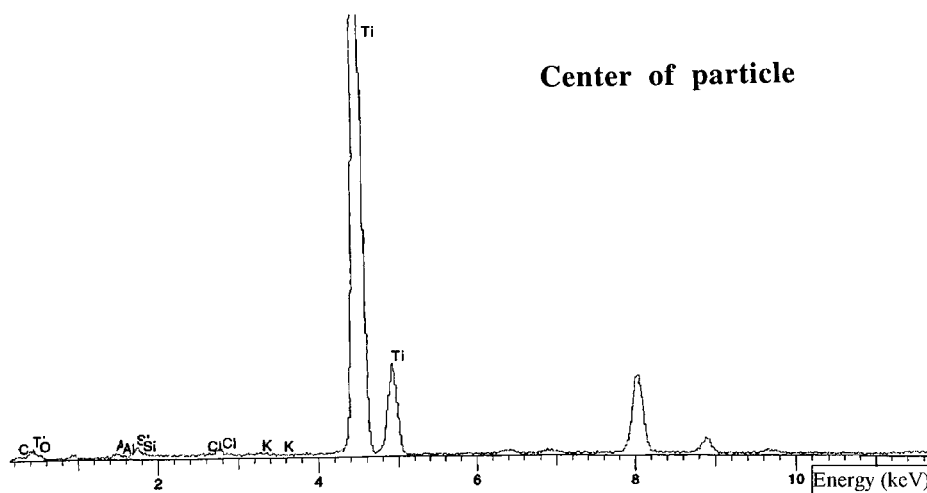
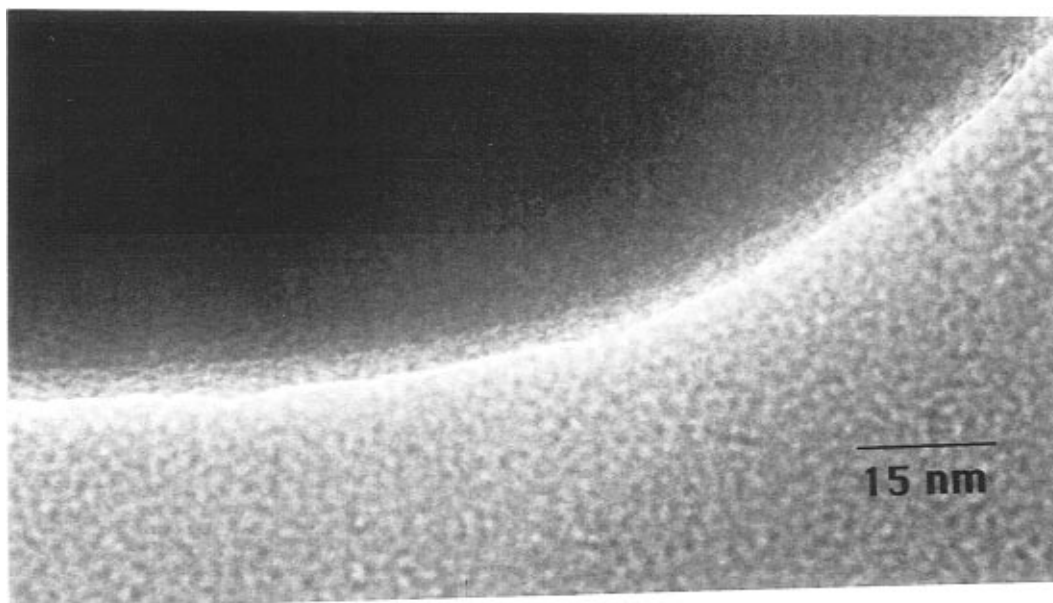


**Figure 6.** (a, top) Titania coated with an approximately 4 nm thick, dense  $\text{Al}_2\text{O}_3/\text{SiO}_2$  layer. This powder was made at 1300 °C using the lowest amount of alumina relative to silica ( $\text{SiO}_2/\text{Al}_2\text{O}_3$  of 10:1). All of the particles made under these conditions had similar coatings which fully encapsulated the particles. (b, bottom) EDS spectra from the center and the edge of an  $\text{Al}_2\text{O}_3/\text{SiO}_2$ -coated  $\text{TiO}_2$  particle which verifies that the surface of the particle was Al and Si rich. This powder was produced using an  $\text{SiO}_2/\text{Al}_2\text{O}_3$  of 10:1, based on inlet conditions.

involved. In the following discussion we will support the proposed coating formation scheme by identifying

individual paths based on physical evidence provided by our experimental observations.

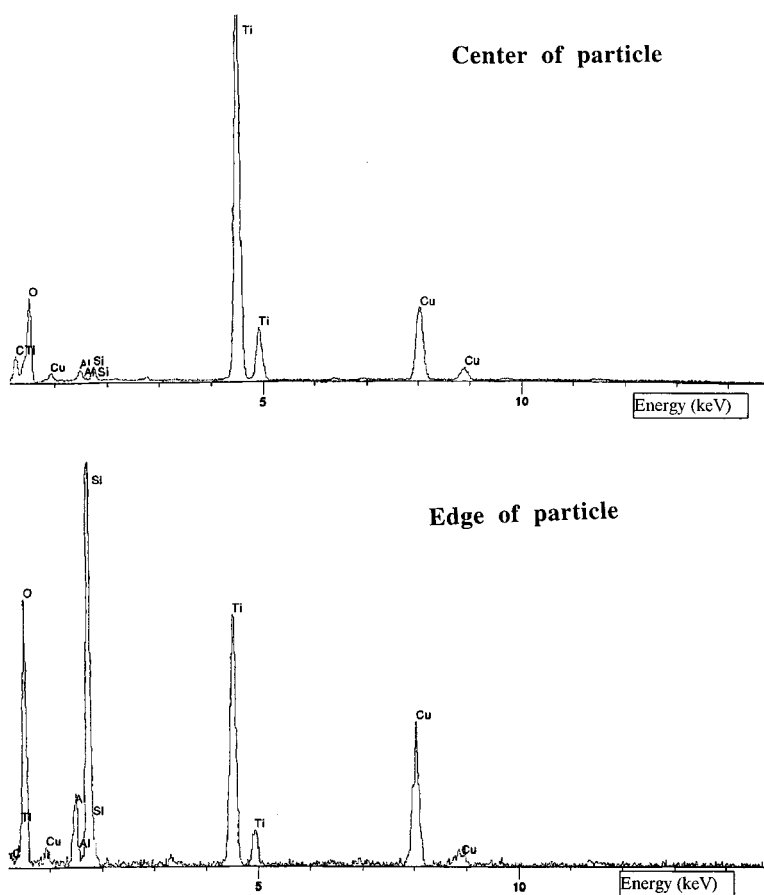
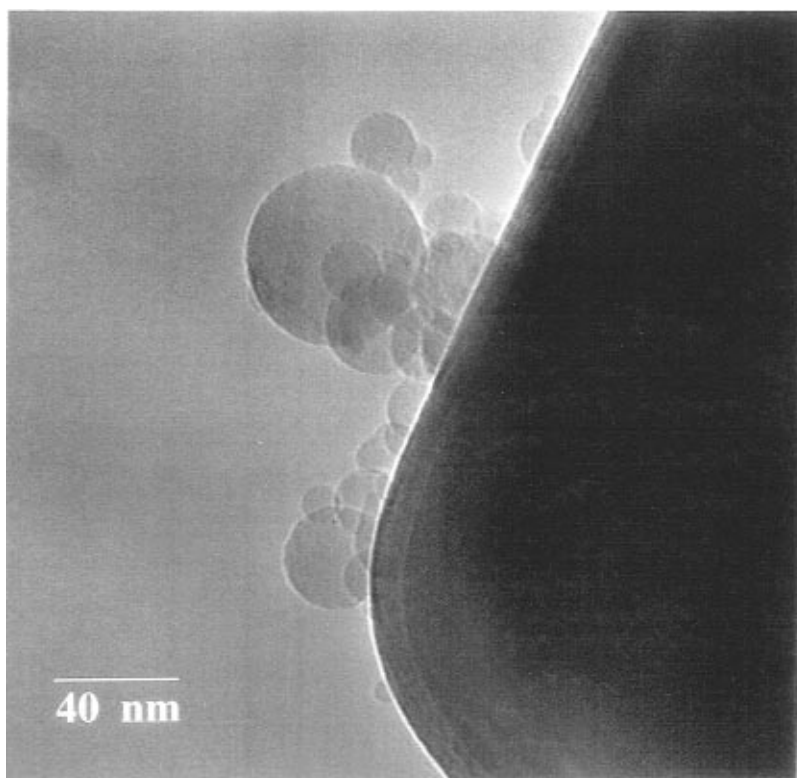


**Figure 7.** (a) Titania coated with an approximately 10 nm thick, dense  $\text{Al}_2\text{O}_3/\text{SiO}_2$  layer and  $\text{Al}_2\text{O}_3/\text{SiO}_2$  particles attached to the surface. These coatings were made at 1300 °C using a moderate amount of alumina relative to silica ( $\text{SiO}_2/\text{Al}_2\text{O}_3$  of 2:1, based on inlet conditions). Not all of the particles had coatings in this powder and the coating thickness varied from particle to particle. (b) EDS spectra from the center and the edge of an  $\text{Al}_2\text{O}_3/\text{SiO}_2$ -coated  $\text{TiO}_2$  particle which verifies that the surface of the particle was Al and Si rich. This powder was produced using an  $\text{SiO}_2/\text{Al}_2\text{O}_3$  of 2:1, based on inlet conditions.

In the alumina-coating experiments when low  $\text{AlCl}_3$  concentrations were used ( $\text{Al}_2\text{O}_3 < 1$  wt % in product

powder), smooth, dense, and uniform coatings were obtained at both 1300 and 1500 °C and no separate

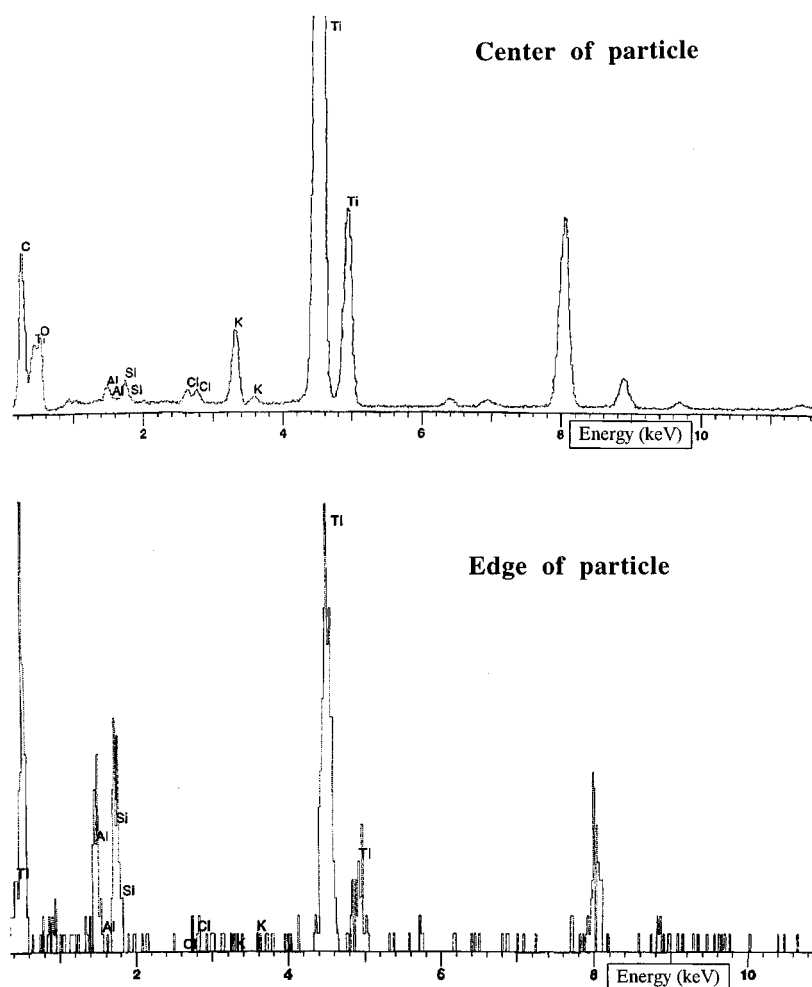
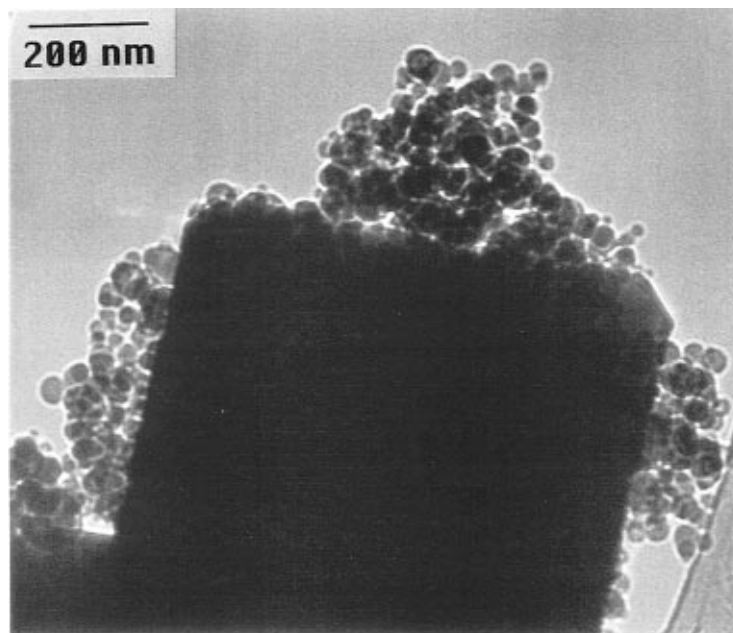


**Figure 8.** (a) Titania particle surrounded by  $\text{Al}_2\text{O}_3/\text{SiO}_2$  particles. This was typical of samples made at  $1300^\circ\text{C}$  using the highest amount of alumina relative to silica ( $\text{SiO}_2/\text{Al}_2\text{O}_3$  of 1:1, based on inlet conditions). Only some of the  $\text{TiO}_2$  particles had dense coatings of  $\text{Al}_2\text{O}_3/\text{SiO}_2$ . (b) EDS spectra from the center and the edge of an  $\text{Al}_2\text{O}_3/\text{SiO}_2$ -coated  $\text{TiO}_2$  particle produced using an  $\text{SiO}_2/\text{Al}_2\text{O}_3$  of 1:1 verifying that, when particles had dense coatings of  $\text{SiO}_2/\text{Al}_2\text{O}_3$ , the surface of the particles were Al and Si rich.

alumina particles were found in the samples. These conditions favored surface reaction of  $\text{AlCl}_3$  vapor on titania according to path 6. It is also likely that some alumina particles were formed (paths 1 and 2). How-

ever, if formed at all, these particles did not grow substantially because of the low  $\text{AlCl}_3$  concentration but coagulated with titania (path 3) and sintered rapidly, thereby forming smooth coatings. The alumina/silica

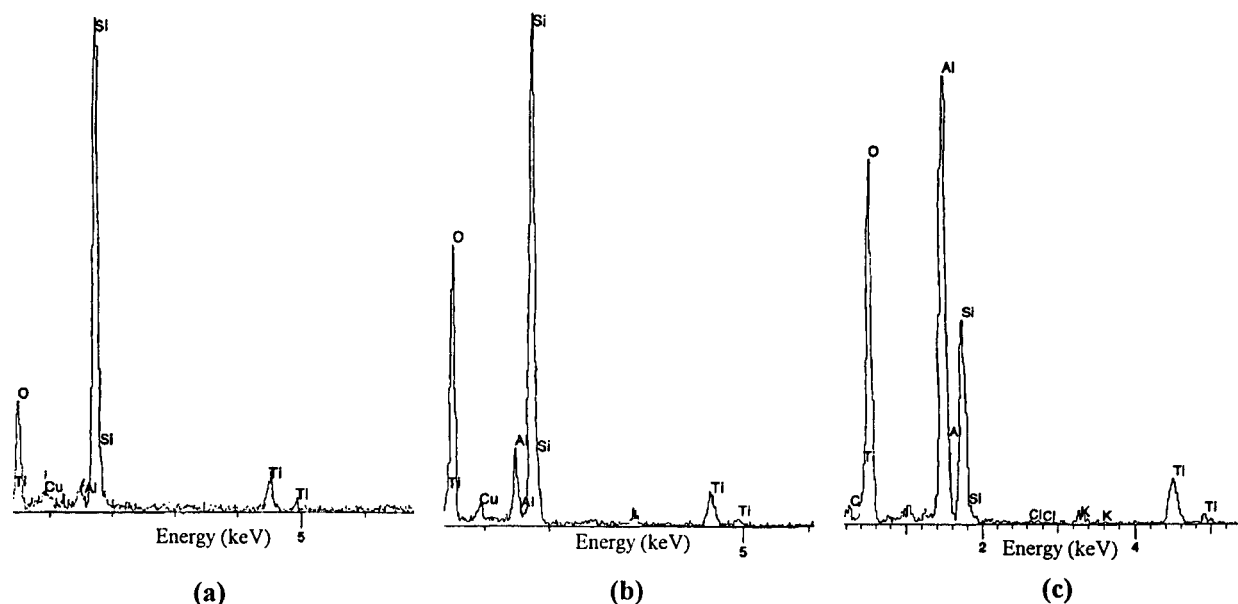


**Figure 9.** Energy-dispersive spectroscopy of mixed  $\text{SiO}_2/\text{Al}_2\text{O}_3$  particles made using  $\text{SiO}_2/\text{Al}_2\text{O}_3$  weight ratios of (a) 6:1, (b) 2:1, and (c) 1:1 showing that as the amount of alumina relative to silica was increased, the amount of alumina relative to silica in particles formed by gas-to-particle conversion during coating increased.

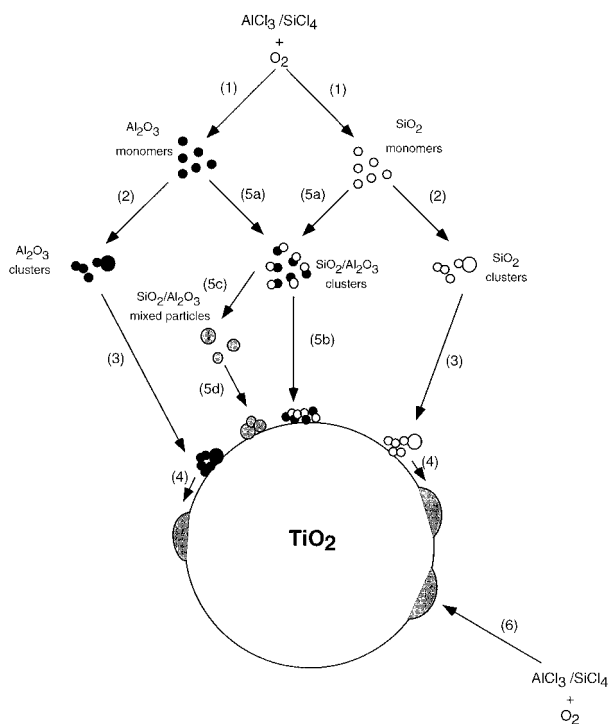


**Figure 10.** Proposed coating mechanism for the  $\text{TiO}_2/\text{Al}_2\text{O}_3/\text{SiO}_2$  system.

system showed a similar behavior at high  $\text{SiO}_2/\text{Al}_2\text{O}_3$  ratios or, equivalently, at low  $\text{AlCl}_3$  concentrations.

At intermediate  $\text{AlCl}_3$  concentrations (1 wt %  $\text{Al}_2\text{O}_3$  < 5 wt % in product powder) or at  $\text{SiO}_2/\text{Al}_2\text{O}_3$  ratios 2 and 6 a variety of titania particle morphologies were obtained. The majority of titania particles were coated with thin alumina or alumina/silica layers (5–10 nm) on top of which there were deposited alumina or alumina/silica particles (Figure 6b). These surface morphologies suggest a combination of surface reaction (path 6) and particle formation and scavenging (paths 1–3). In the case of alumina/silica coatings, the composite silica/alumina particles seen on the  $\text{TiO}_2$  surfaces resulted from paths 1, 5a, 5c, and 5d. Their composition

followed the changes in chemical composition of the feed gas stream as Figure 9 shows. No separate alumina or silica particles were detected in this case that could have formed by paths 1 and 2. Apparently, premixing the  $\text{AlCl}_3$  and  $\text{SiCl}_4$  vapors in the feed stream results in homogeneity at a molecular level which is reflected in the homogeneous composition of the resulted coating particles and layers.

At the highest  $\text{AlCl}_3$  concentrations ( $\text{Al}_2\text{O}_3$  < 5 wt % in product powder) and lowest  $\text{SiO}_2/\text{Al}_2\text{O}_3$  ratio (1:1) used in this study coating by particle scavenging prevailed (paths 1–3 or 1, 5a, 5c, and 5d). The  $\text{AlCl}_3$  and  $\text{SiCl}_4$  vapors were consumed mostly by gas-phase particle formation, and surface reaction (path 6) may have been suppressed. The formation of separate and larger silica–alumina particles in contrast to the chain-like silica aggregates obtained in the silica–titania system<sup>8</sup> is attributed to the higher reactivity of  $\text{AlCl}_3$  relative to  $\text{SiCl}_4$ . Suyama and Kato reported activation energies for the reaction of  $\text{AlCl}_3$  and  $\text{SiCl}_4$  as 25 and 90 kcal/mol, respectively.<sup>10</sup> For the same chloride concentration, the faster gas-phase reaction rate of  $\text{AlCl}_3$  translates to higher initial number concentration of alumina monomers which leads to the formation of larger alumina particles by coagulation and sintering. The nonuniformity of the coatings and the presence of a significant number of uncoated titania particles at these conditions are attributed to nonuniform mixing in the coating section of the reactor where laminar flow conditions existed. Moreover, the smaller diffusion coefficients of the larger alumina or alumina/silica particles formed under these conditions resulted in lower collision rates with the titania particles which translated to less efficient scavenging.<sup>11</sup> This led to the collection of uncoated titania particles and more separate alumina or alumina/silica particles.

At low  $\text{Al}_2\text{O}_3$  levels the behavior of the  $\text{TiO}_2/\text{Al}_2\text{O}_3/\text{SiO}_2$  system resembled that of the  $\text{TiO}_2/\text{SiO}_2$  system

(10) Suyama, Y.; Kato, A. *J. Am. Ceram. Soc.* **1976**, *59*, 146.

(11) Friedlander, S. K.; Koch, W.; Main, H. H. *J. Aerosol Sci.* **1991**, *22*, 1.



studied earlier.<sup>8</sup> Nevertheless, the addition of small amounts of alumina rendered the coatings denser, smoother and more compact (Figure 6a, Figure 5 in ref 8). It is known that the presence of certain metals or metal oxides enhances the sintering rate of silica.<sup>12,13</sup> On the other hand, the sintering rate of alumina is enhanced in the presence of titania.<sup>14</sup> It is possible that alumina affects the sintering behavior of silica. This suggests that alumina can possibly serve as a coating morphology control agent in the silica/alumina system under certain conditions.

### Conclusions

Titania particles formed by an aerosol process were coated in situ in a continuous flow reactor with  $\text{Al}_2\text{O}_3$  and  $\text{SiO}_2/\text{Al}_2\text{O}_3$ . Low  $\text{Al}_2\text{O}_3$  mass loadings (<1 wt %) resulted in smooth and dense coatings 5–20 nm thick. At higher  $\text{Al}_2\text{O}_3$  mass loadings, separate  $\text{Al}_2\text{O}_3$  particles were formed and were partially scavenged by the titania particles. A similar trend was observed in the  $\text{Al}_2\text{O}_3/\text{SiO}_2$ -coated titania. The above observations suggest that  $\text{Al}_2\text{O}_3$  and  $\text{Al}_2\text{O}_3/\text{SiO}_2$  coatings were formed on titania by surface reaction of  $\text{AlCl}_3$  and  $\text{SiCl}_4$  vapors (smooth coatings) and by coagulation with  $\text{Al}_2\text{O}_3$  and/

or  $\text{Al}_2\text{O}_3/\text{SiO}_2$  particles formed by gas-phase reaction (rough coatings). The relative rates of surface reaction and gas-phase reaction of the coating precursors ( $\text{AlCl}_3$  and  $\text{SiCl}_4$ ) as well as the mixing of these precursors with the titania particles in the coating region determined to a great extent the morphology of the coated particles. These rates strongly depended on the chloride concentration in the reactor and were not affected by the reactor temperature in the range 1300–1500 °C. Deposition rates up to 50 nm/s were achieved with this coating process. Overall, these results suggest that aerosol reactors for coating should be designed to have high  $\text{TiO}_2$  particle surface area, high temperature relative to the sintering temperatures of  $\text{SiO}_2$ ,  $\text{Al}_2\text{O}_3$  and  $\text{SiO}_2/\text{Al}_2\text{O}_3$ , and addition of  $\text{Al}_2\text{O}_3$  to  $\text{SiO}_2$  to lower coating densification temperature.

**Acknowledgment.** We would like to thank Dr. Lu Min Wang of the Earth and Planetary Sciences Department at the University of New Mexico for providing access to the high-resolution transmission electron microscopes and Dr. Mark Hampden-Smith of the Chemistry Department at the University of New Mexico for the use of the X-ray diffractometer. This work was supported by Kemira Pigments, Inc. T.T.K. acknowledges matching funds from the National Science Foundation Presidential Young Investigator Award CTS-9058538.

CM960334G

(12) Zachariah, M. R.; Shull, R. D.; McMillin, B. K.; Biswas, P. *Nanotechnology, Am. Chem. Soc. Symp. Ser.* **1996**, *622*, 42–63.

(13) Fotou, G. P.; Scott, S. J.; Pratsinis, S. E. *Combust. Flame* **1995**, *101*, 529.

(14) Bagley, R. D.; Cutler, I. B.; Johnson, D. L. *J. Am. Ceram. Soc.* **1970**, *53*, 136.